

Modeling SEDs and light curves of BL Lacertae using a time-dependent shock-in-jet model



Rukaiya Khatoon & Markus Boettcher

Centre for Space Research, North-West University, Potchefstroom, 2520, South Africa

Email: rukaiyakhatoon12@gmail.com

Abstract

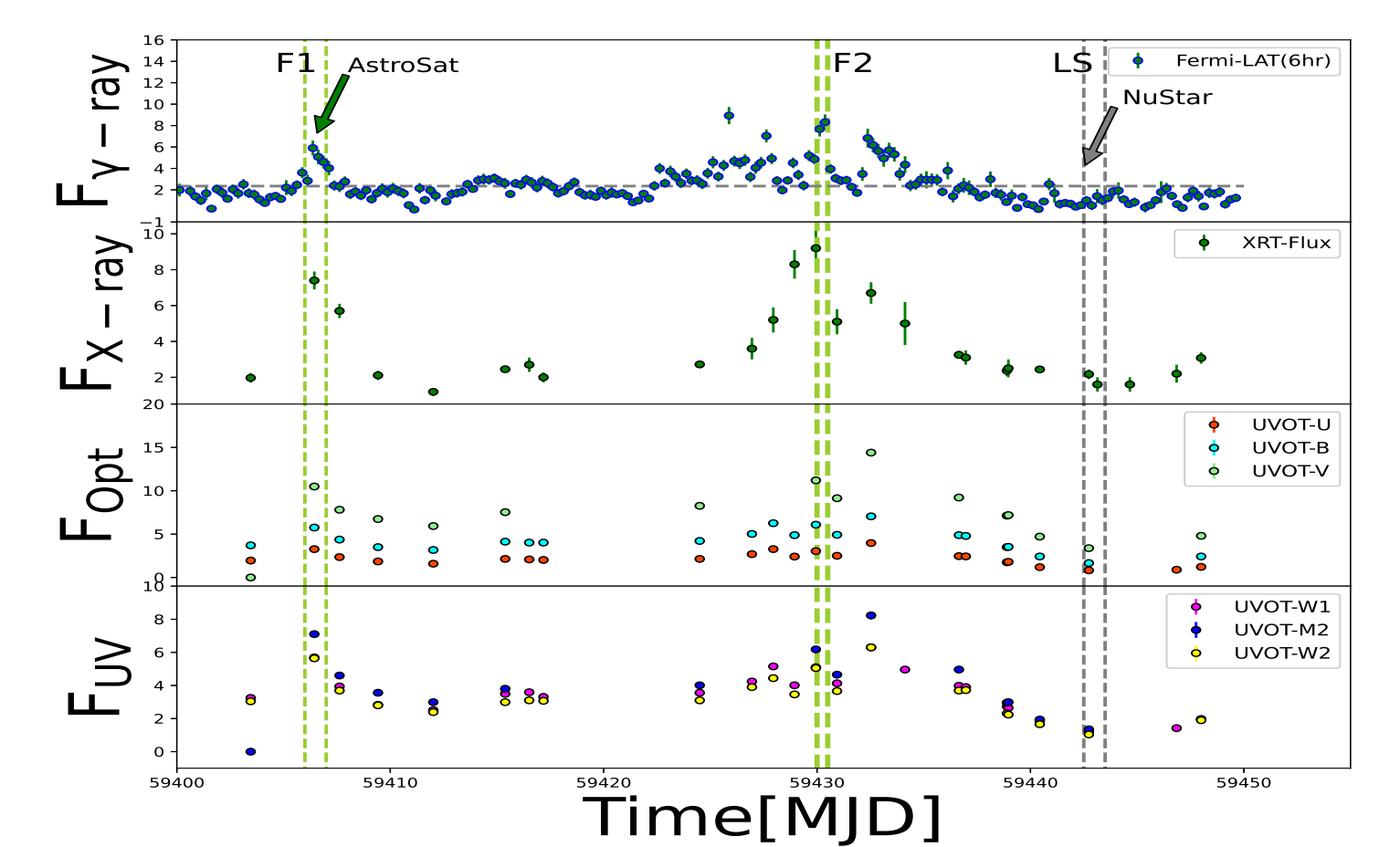
This study focuses on BL Lacertae, modeling its spectral energy distributions (SEDs) and broadband light curves using a diffusive shock acceleration process with multiple mildly relativistic shocks and a time-dependent radiation transfer process. It uses simultaneous observations across optical-UV frequencies with Swift-UVOT, X-rays with Swift-XRT and AstroSat-SXT/LAXPC, and gamma-rays with Fermi-LAT, covering the period from July to August 2021. Modeling simultaneously the SEDs and the multiband light curves provides insights into the particle acceleration mechanisms at play.

Introduction

BL Lacertae stands as the prototype of the BL Lac class of blazars, with a relativistic jet oriented close to the line of sight of the observer. The broadband SED of blazars displays two distinct peaks. The origin of the low-energy component is attributed to synchrotron emission, which arises from relativistic electrons spiraling around magnetic fields within the jet. Conversely, the high-energy component is often modeled as inverse-Compton (IC) scattering, where relativistic electrons interact with low-energy photons. These low-energy photons may originate either internally (through synchrotron emission) or externally (from sources like the accretion disk, broad-line region, dusty torus, etc.) to the jet. BL Lacertae, at a redshift of $z = 0.069$, experienced a multi-wavelength outburst in early July 2021. In this study, we perform a comprehensive investigation of the spectral and light curve characteristics of the source utilizing data obtained from Fermi-LAT, NuStar, Swift-XRT/UVOT and AstroSat-SXT/LAXPC, respectively.

Multiwavelength lightcurves:

The multiband light curves of BL Lac over ~ 50 days (MJD 59400-59450) show flux variations across all wavebands, with both high and low flux states. The figure panels, from top to bottom, represent gamma-ray, X-ray, optical, and UV observations. The top panel's grey dashed line indicates the average gamma-ray flux ($F_a = 2.35 \times 10^{-6} \text{ phcm}^{-2} \text{ s}^{-1}$) from 6-hour binned data. High flux states, where gamma-ray flux exceeds F_a , are marked by green dashed lines, while low flux states (below F_a) are marked by grey dashed lines. In high-flux states, the source shows increased flux in X-ray, optical, and UV bands, while in the low-flux state, it displays low flux across all wavebands. We modeled the SED during both high and low-flux states. To illustrate the capability of the shock-in-jet model to reproduce both snapshot SEDs and light curve segments, we focused the modeling of light curves on the period from MJD 59400 to MJD 59420.



Modeling of SEDs and Lightcurves

The time-dependent shock-in-jet model incorporates hybrid thermal and nonthermal electron spectra generated through Monte Carlo simulations of diffusive shock acceleration by mildly relativistic shocks. The MC simulations of diffusive shock acceleration parameterize the electrons' mean free path to pitch-angle scattering (PAS) as $\lambda_{pas} = \eta_0 r_g p^{\alpha-1}$, where r_g denotes the gyroradius of an electron, and p representing its momentum. The parameters η_0 and α are derived from the simulations. The SED and lightcurves are primarily governed by the shock parameters η_0 and α , the power dissipated by the shock and transferred to relativistic electrons (referred to as "injection luminosity", L_{inj} hereafter), the strength of the magnetic field (B), the bulk Lorentz factor Γ , and the radius R of the emission region.

1. SED modeling:

We begin the SED fitting process by configuring a quiescent state to reproduce the low-state SED of BL Lacertae, allowing the code to reach equilibrium with constant shock acceleration parameters. Using these parameters, we then model SED for the high-state by varying the shock-acceleration parameters over time and extracting snapshot SEDs during these changes.

Model fit parameters to SEDs

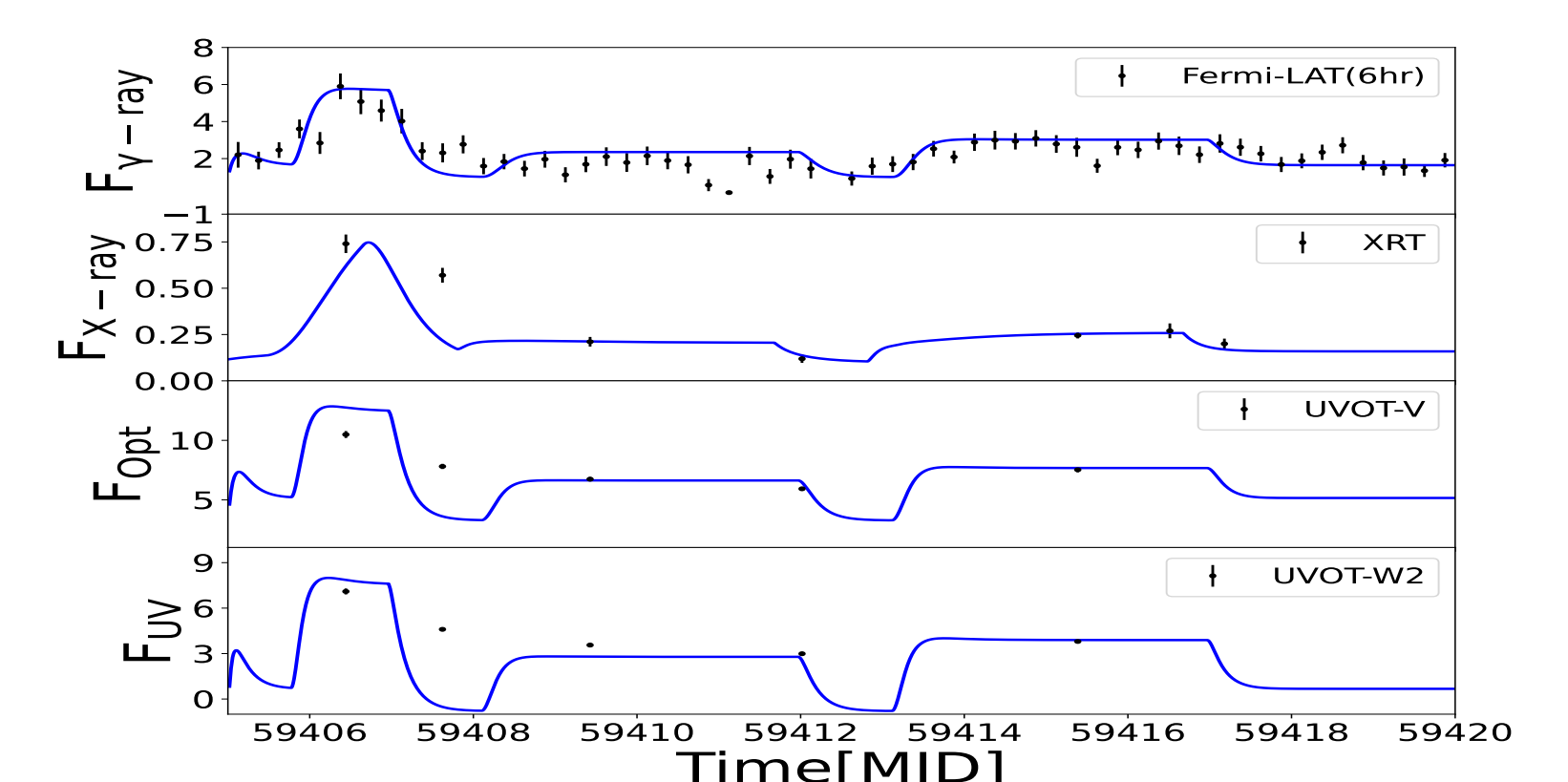
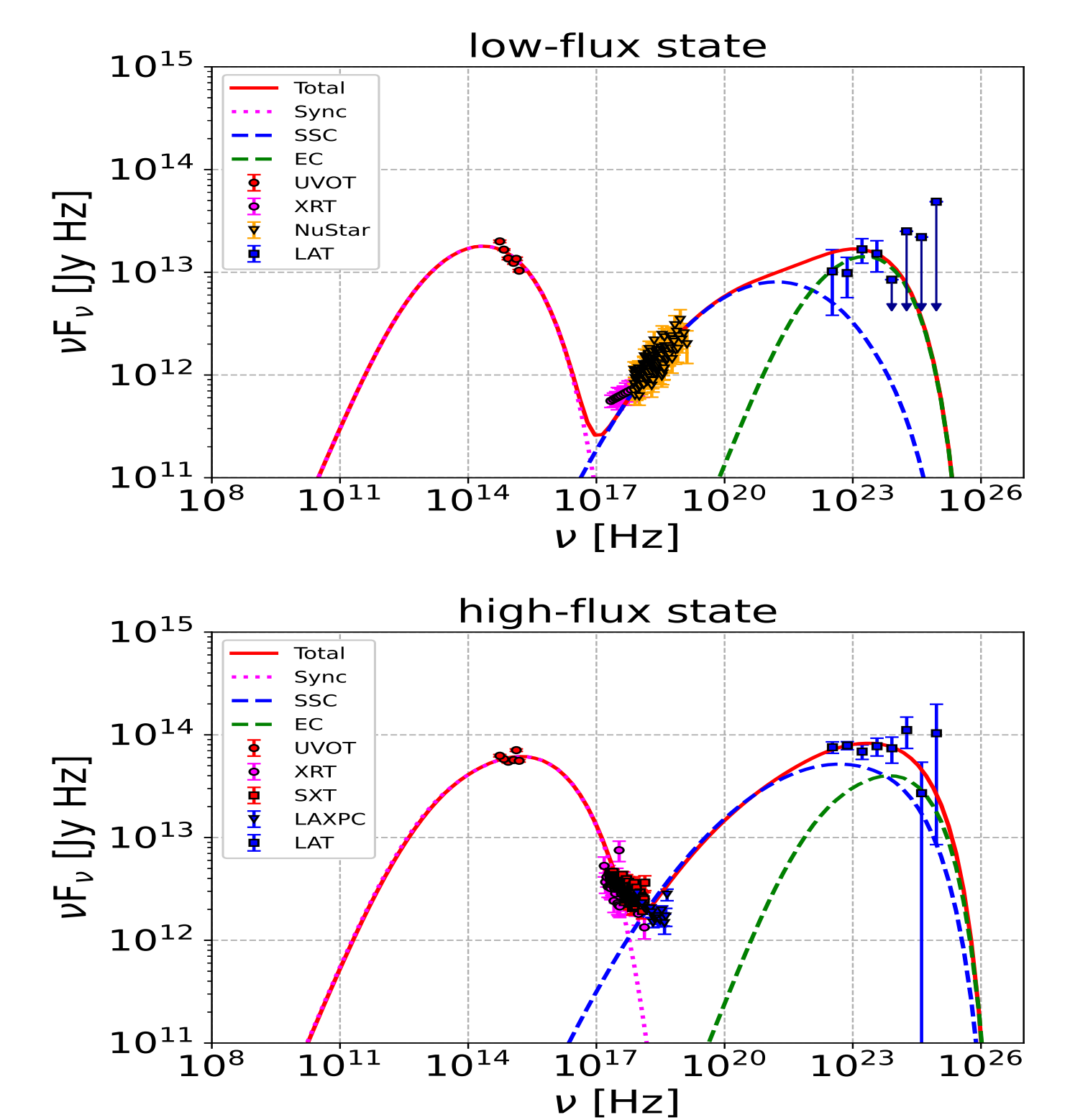
Name	Symbol/units	LS	HS
Injection mean free path	η_0	30	40
Diffusion index	α	3.0	2.5
Electron injection luminosity	L_{inj} [erg/s]	3.3×10^{41}	1.2×10^{42}
Magnetic field	B [G]	0.75	0.75
Emission region size	R [cm]	1.0×10^{16}	1.0×10^{16}

2. Lightcurve modeling:

The light curve modeling starts with the quiescent state configuration (see Table & Figure in section 1) as the reference low state of the initial outburst. To fit the subsequent outbursts, we adjust the shock parameters.

Parameter variations for the fits to MWL light curves.

Parameter [units]	L_{inj} [erg/s]	η_0	α
Quiescence	3.3×10^{41}	30	3.0
Shock 1	2.4×10^{42}	30	2.8
Shock 2	5.5×10^{41}	30	2.5
Shock 3	8.0×10^{41}	30	2.5



Results and Interpretations

- The primary change between low and high flux states is the hardening of the electron spectrum due to a significant change in the PAS mean-free-path momentum-scaling index, α . Additionally, an increase in the injection luminosity L_{jet} is required.
- Multi-wavelength flares may result from turbulence generated by shocks, reducing the mean free path of electrons for pitch-angle scattering (λ_{pas}), as indicated by a slight decrease in the value of α , enhancing particle acceleration efficiency. An increase in particle injection luminosity, along with minor variations in magnetic field strength, also contributes to flux enhancements.